

PhICNet: Physics-Incorporated Convolutional Recurrent Neural Networks for Modeling Dynamical Systems

Priyabrata Saha¹ Saurabh Dash¹ Saibal Mukhopadhyay¹

Abstract

Dynamical systems involving partial differential equations (PDEs) and ordinary differential equations (ODEs) arise in many fields of science and engineering. In this paper, we present a physics-incorporated deep learning framework to model and predict the spatiotemporal evolution of dynamical systems governed by partially-known inhomogeneous PDEs with unobservable source dynamics. We formulate our model PhICNet as a convolutional recurrent neural network which is end-to-end trainable for spatiotemporal evolution prediction of dynamical systems. Experimental results show the long-term prediction capability of our model.

1. Introduction

Understanding the behavior of dynamical systems is a fundamental problem in science and engineering. Classical approaches of modeling dynamical systems involve formulating ordinary or partial differential equations (ODEs or PDEs) based on various physical principles like conservation laws, profound reasoning, intuition, knowledge and verifying those with experiments and observations. Recent successes of machine learning methods in complex sequence prediction tasks along with development in sensor technologies and computing systems motivate to predict the evolution of dynamical system directly from observation data without rigorous formalization and experiments by human experts (Sutskever et al., 2014; Chung et al., 2014; Xingjian et al., 2015; Finn et al., 2016; Kumar et al., 2016; Lee et al., 2017; Minderer et al., 2019). Consequently, a number of machine learning models which incorporate knowledge from physics or applied mathematics, have been introduced for modeling complex dynamical systems (Schaeffer, 2017; Rudy et al., 2017; Raissi, 2018; Long et al., 2018b;a; de Bezenac et al., 2019).

¹School of Electrical and Computer Engineering, Georgia Tech, Atlanta, USA. Correspondence to: Priyabrata Saha <priyabratasaha@gatech.edu>.

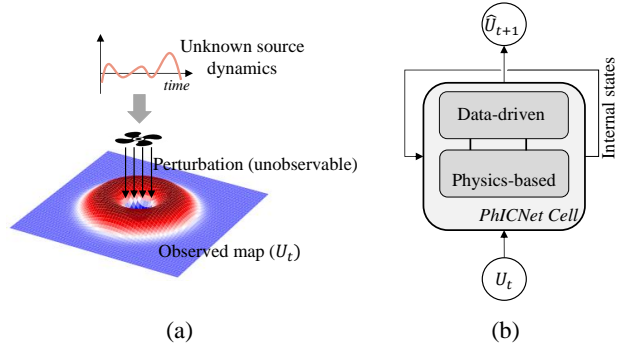


Figure 1. (a): An example dynamical system governed by partially-known PDE and unknown source dynamics. (b): High-level diagram of the recurrent network cell that is used to model such dynamics. Unobservable perturbation is learned as an internal state of PhICNet cell.

Real-world dynamical systems are often subjected to perturbation from time-varying external sources. Figure 1(a) shows an example where an elastic membrane under tension is being perturbed with an independent time-varying pressure. The undulation of the membrane can be observed as a regularly sampled spatiotemporal sequence. However, the spatiotemporal variation in the source term is often not known and not observable; but it couples with the wave propagation system to determine the undulation in the membrane. Moreover, although the basic governing dynamics (wave equation) of the system is known, the physical parameters such as propagation speed in that particular medium are often unknown. In such scenarios, we need to be able to predict spatiotemporal evolution of dynamical systems from partial knowledge of the governing dynamics and limited observability of the factors that influence the system behaviors.

In this paper, we consider to model a generic PDE-based dynamical system which is perturbed with external sources that follow another independent dynamics. Our goal is to design a neural network model that can be used for long-term prediction of the entire systems, as well as of the source dynamics. We assume the physical quantity that follows the combined dynamics can be observed as regularly sampled spatiotemporal sequence, but the source or perturbation is

not observable separately. It is further assumed that we know what type of system we are observing and therefore scientific knowledge of such system can be incorporated in the model. In particular, we assume that the analytical form the underlying PDE is known a priori, *but the physical parameters of the system are unknown*.

We propose **Physics-Incorporated Convolutional Recurrent Neural Networks** (PhICNet) that combine physical models with data-driven models to learn the behavior of dynamical systems with unobservable time-varying external source term. Figure 1(b) shows the high-level diagram of a PhICNet cell. The basic concept of PhICnet is based on two key contributions. First, a generic homogeneous PDE of any temporal order can be mapped into a recurrent neural network (RNN) structure with trainable physical parameters. Second, the basic RNN structure for homogeneous PDE can be modified and integrated with a residual encoder-decoder network to identify and learn the source dynamics. The RNN structure stores the homogeneous solution of the underlying PDE as an internal state which is then compared with the input (observation) at the next step to find out if there exists some source term or perturbation. The residual encoder-decoder network learns to propagate the source term as it is in case of constant perturbation or predict its progress in case of dynamic perturbation. The PhICNet cell stores the estimated perturbation or source term as an internal cell which can be used to understand behaviour of source dynamics. The integrated model can be trained end-to-end using stochastic gradient descent (SGD) based backpropagation through time (BPTT) algorithm.

Few existing models in literature can be used or extended to perform the spatiotemporal sequence prediction of dynamical systems with time-varying independent source. Pure data-driven models like ConvLSTM (Xingjian et al., 2015), residual networks (He et al., 2016; Mao et al., 2016) can be used directly, but these models lack consideration of underlying physical dynamics resulting in limited accuracy. Furthermore, these pure data-driven models cannot identify the source dynamics separately. Deep hidden physics models (DHPM) (Raissi, 2018) can model the underlying homogeneous PDE, but does not consider any nonlinear source term. A polynomial approximation can be added in DHPM to model nonlinear internal source. This strategy is used in PDE-Net (Long et al., 2018b) to incorporate nonlinear source term. Although they consider only internal source term that is a nonlinear function of the observed physical quantity, we discuss later a minor modification will allow us to extend the model to consider independent source dynamics. DHPM, PDE-Net only consider PDEs that are first-order in time, although can be extended to model higher temporal order systems if we know the temporal order a priori.

Our approach fundamentally differs from the past approaches as we model the system as an RNN that couples the known and unknown dynamics within the hidden cells and enables end-to-end training. We evaluate our model along with other baselines for two types dynamical systems: a heat diffusion system and a wave propagation system. Experiments show that our model provides more accurate prediction compared to the baseline models. Furthermore, we show that our model can predict the source dynamics separately which is not possible with other models.

2. Related Work

2.1. RNNs for Dynamical Systems

Several studies have interpreted RNNs as approximation of dynamical systems (Funahashi & Nakamura, 1993; Li et al., 2005; Liao & Poggio, 2016; Chen et al., 2018). Recently, a number of RNN architectures have been proposed for data-driven modeling of dynamical systems. Trischler & DEleuterio (2016) proposed an algorithm for efficiently training RNNs to replicate dynamical systems and demonstrated its capability to approximate attractor dynamical systems. A class of RNNs, namely Tensor-RNNs, has been proposed in (Yu et al., 2017a;b) for long-term prediction of nonlinear dynamical systems. Yeo & Melnyk (2019) use LSTM for long-term prediction of nonlinear dynamics.

2.2. Learning PDEs from Data

Recently, numerous attempts have been made on data-driven discovery of PDE-based dynamical systems. Schaeffer (2017); Rudy et al. (2017) use sparse optimization techniques to choose the best candidates from a library of possible partial derivatives of the unknown governing equations. Raissi & Karniadakis (2018) proposed a method to learn scalar parameters of PDEs using Gaussian process. A deep neural network is introduced in (Raissi et al., 2017) to approximate the solution of a nonlinear PDE. The predicted solution is then fed to a physics-informed neural network to validate that solution. The physics-informed neural network is designed based on the explicit form of the underlying PDE which is assumed to be known except for a few scalar learnable parameters. Raissi (2018) extended (Raissi et al., 2017) to replace the known PDE-based neural network to a generalized neural network which discovers the dynamics of underlying PDE using predicted solution and its derivatives. The inputs of the neural network are the partial derivatives up to a maximum order which is considered as a hyperparameter. Long et al. (2018b) introduced PDE-Net that uses trainable convolutional filters to perform differentiations. Filters are initialized as differentiating kernels of corresponding orders, and trained by imposing some constraints to maintain differentiating property. They assumed that the maximum order of derivative is known a priori. In

PDE-Net 2.0 (Long et al., 2019), a symbolic neural network is integrated with original PDE-Net to uncover more complex analytical form. de Bezenac et al. (2019) proposed a convolutional neural network (CNN) that incorporates prior scientific knowledge for the problem of forecasting sea surface temperature. They design their model based on the general solution of the advection-diffusion equation. Long et al. (2018a) studied a problem similar to ours where the source or perturbation term of the PDE follows another dynamics. They mapped the known PDE into a cellular neural network with trainable physical parameters and integrate that with ConvLSTM (Xingjian et al., 2015) that models the source dynamics. However, they assumed that the source or perturbation is observable and they train the two networks separately.

3. Problem Description

We consider dynamical systems governed by the following generic inhomogeneous PDE

$$\frac{\partial^n u}{\partial t^n} = F\left(x, y, u, \frac{\partial u}{\partial x}, \frac{\partial u}{\partial y}, \frac{\partial^2 u}{\partial x^2}, \frac{\partial^2 u}{\partial x \partial y}, \frac{\partial^2 u}{\partial y^2}, \dots; \theta\right) + v(x, y, t), \quad (x, y) \in \Omega \subset \mathbb{R}^2, t \in [0, T]. \quad (1)$$

$u(x, y, t) \in \mathbb{R}$ is the observed physical quantity at the spatial location $(x, y) \in \Omega$ at time $t \in [0, T]$. θ corresponds to the physical parameters of the system. For example, if we are studying a diffusive system, then θ corresponds to the diffusivity of the medium. $v(x, y, t) \in \mathbb{R}$ is the source term or perturbation at location $(x, y) \in \Omega$ at time $t \in [0, T]$ which is governed by another independent first order dynamics delineated by:

$$\frac{\partial v}{\partial t} = G(x, y, v) \quad (2)$$

Our goal is to predict the spatiotemporal evolution of the system jointly defined by equation 1 and equation 2.

Assumptions We make following assumptions about the problem:

- We have the a priori knowledge about what type of physical quantities we are observing and how such system behave in absence of any external perturbation or source. In other words, we know the analytical form of function F and the temporal order n .
- Physical parameters of the system θ are not known to us.
- The source term is constant or follows an unknown first order (temporal) dynamics. The perturbation v is not observable or cannot be computed directly from the observed quantity u as θ are unknown.

This problem can be formulated as a spatiotemporal sequence prediction problem. Suppose the observation space

is discretized into a $X \times Y$ grid and $U_t \in \mathbb{R}^{X \times Y}$ is the observed map at timestep $t \in \{0, 1, \dots, T\}$. We aim to design a physics-incorporated convolutional-RNN \mathcal{R} :

$$\hat{U}_{t+1} = \mathcal{R}(\hat{U}_t, \dots, \hat{U}_{t-n}), \quad t \in \{n, \dots, T-1\} \quad (3)$$

such that $\sum_{t=n+1}^T \mathcal{L}(U_t, \hat{U}_t)$ is minimized. \hat{U}_t is the predicted map at timestep $(t-1)$ and $\hat{U}_t = U_t \quad \forall t \in \{0, \dots, n\}$. \mathcal{L} is the loss function between observed map and predicted map. It is noteworthy that we need $(n+1)$ previous maps, instead of just n , to predict the next map in an n^{th} order (temporal) system because the source/perturbation is unknown and source follows an first order dynamics.

4. The PhICNet Model: Foundation and Design

4.1. Background on Recurrent Neural Networks

The recurrent neural network (RNN) is an elegant generalization of feedforward neural networks to incorporate temporal dynamics of data (Rumelhart et al., 1986; Werbos, 1990; Schuster & Paliwal, 1997). The RNN and its various evolved topologies have proven efficacious in numerous sequence modelling tasks (Pearlmutter, 1989; Robinson, 1994; Hochreiter & Schmidhuber, 1997; Sutskever et al., 2014; Xingjian et al., 2015). At each time step, an input vector i_t is fed to the RNN. The RNN modifies its internal state h_t based on the current input and previous internal state. The updated internal state is then used to predict the output o_t . The following set of equation (equation 4) delineates the computation inside a standard RNN.

$$\begin{aligned} h_t &= \sigma_h(W_{hi}i_t + W_{hh}h_{t-1} + b_h) \\ o_t &= \sigma_o(W_{oh}h_t + b_o) \end{aligned} \quad (4)$$

W_{hi}, W_{hh}, W_{oh} are the weight matrices of the RNN and b_h, b_o are bias vectors. σ_h and σ_o are activation functions like *sigmoid*, *tanh*. Temporal update in the internal state allows the RNN to make use of past information while predicting the current output.

The input i_t , internal state h_t and output o_t of standard RNN are all 1D vectors and the operations are fully-connected. To deal with 2D image data, Xingjian et al. proposed convolutional LSTM (Xingjian et al., 2015) that uses convolutional operations instead of fully-connected operations of standard LSTM (Hochreiter & Schmidhuber, 1997), an evolved variant of the RNN. Incorporating convolutional operations in RNN, we can write the computation inside a convolutional-RNN as follows:

$$\begin{aligned} H_t &= \sigma_h(W_{hi} * I_t + W_{hh} * H_{t-1} + b_h) \\ O_t &= \sigma_o(W_{oh} * H_t + b_o) \end{aligned} \quad (5)$$

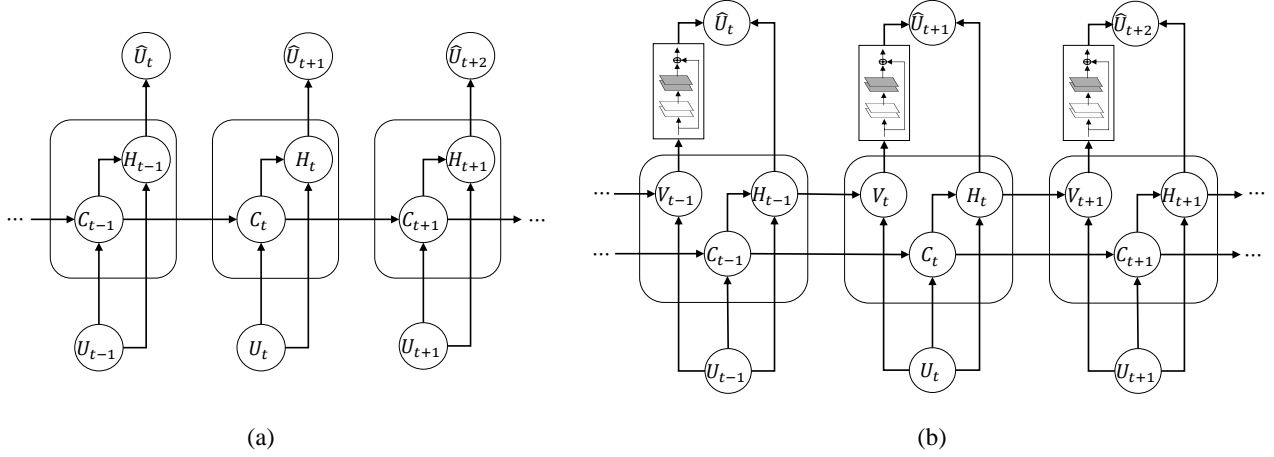


Figure 2. (a): Proposed RNN structure (unfolded) that maps a generic homogeneous PDE. U_t is the observed map at time step t and \hat{U}_{t+1} is the prediction of the next map. H_t and C_t are internal states of the RNN representing the homogeneous solution and cell memory, respectively. For homogeneous PDE, $\hat{U}_{t+1} = H_t$. (b): PhICNet: Proposed RNN structure that models the dynamical system with time-varying independent source. A residual encoder-decoder network, which models the source dynamics, is integrated with (a). V_t stores the estimated perturbation.

where, I_t , H_t and O_t are the input, internal state and output, respectively, of the convolutional-RNN at time step t and are all 2D images. ‘*’ denotes the convolution operator.

4.2. Proposed RNN Model for Generic Homogeneous PDE

Figure 2(a) illustrates the structure of the RNN we propose for modeling a generic homogeneous PDE (i.e. zero source term). Inputs to the RNN cell are 2D observation maps $U_t \in \mathbb{R}^{X \times Y}$, $t \in \{0, \dots, T\}$. The RNN cell keeps an memory that stores the past information required for current step prediction. The concept of cell memory was introduced in LSTM (Hochreiter & Schmidhuber, 1997). Cell memory in LSTM is controlled by several self-parameterized gates to learn what information to store and what information to forget. In contrast, past information required to be stored in the cell memory in our physics-incorporated RNN is completely determined beforehand based on the known temporal order n (in equation 1) of the observed system. For an n^{th} order (temporal) system, the cell memory stores the current and past $(n - 1)$ observed maps. At time step t , the state of the cell memory (we will call it cell state from now on) C_t defined by the following equation

$$C_t = [U_t, \dots, U_{t-n+1}] \quad (6)$$

where $[\cdot]$ denotes the concatenation operation along a new dimension. The cell state can be seen as a 3D tensor ($C_t \in \mathbb{R}^{n \times X \times Y}$). Cell state at current time step t can be written as a function of previous cell state C_{t-1} and current input U_t :

$$C_t = W_{cc} \odot C_{t-1} + w_{cu} \circ U_t \quad (7)$$

W_{cc} is a 2D square matrix of order n and the $(p, q)^{th}$ element of W_{cc} , $p \in \{1, \dots, n\}$ and $q \in \{1, \dots, n\}$, is defined as follows.

$$W_{cc}^{pq} = \begin{cases} 1 & \text{if } p = q + 1, q > 1 \\ 0 & \text{otherwise} \end{cases} \quad (8)$$

‘ \odot ’ denotes a matrix-tensor product resulting in a tensor $\tilde{C} \in \mathbb{R}^{n \times X \times Y}$ such that

$$\tilde{C}^p = \sum_{q=1}^n W_{cc}^{pq} C_{t-1}^q, \quad p \in \{1, \dots, n\}. \quad (9)$$

The operator \circ between 2D observation map $U_t \in \mathbb{R}^{X \times Y}$ and 1D vector $w_{cu} = [1, 0, \dots, 0]^T \in \mathbb{R}^n$ performs a vector-matrix product to yield a tensor $\dot{C} \in \mathbb{R}^{n \times X \times Y}$ such that

$$\dot{C}^p = w_{cu}^p U_t, \quad p \in \{1, \dots, n\}. \quad (10)$$

Cell state C_t and input U_t are used to compute $H_t \in \mathbb{R}^{X \times Y}$ as follows.

$$H_t = w_{hc} \odot C_t + f(U_t, D_{10} * U_t, D_{01} * U_t, D_{11} * U_t, \dots; \theta) \quad (11)$$

$w_{hc} \in \mathbb{R}^n$ is determined by the temporal order of the dynamics. The elements of w_{hc} are the coefficients of past observation maps in the finite difference approximation of $\frac{\partial^n}{\partial t^n}$ and are given by the following equation.

$$w_{hc}^p = (-1)^{p+1} \binom{n}{p}, \quad p \in \{1, \dots, n\} \quad (12)$$

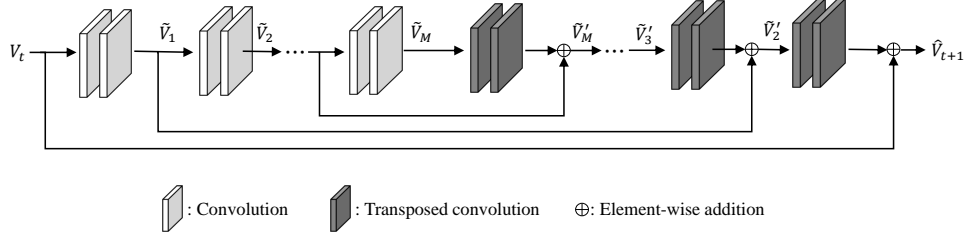


Figure 3. Architecture of the residual encoder-decoder network used for source dynamics modeling.

‘ \odot ’ denotes a vector-tensor product resulting in a 2D matrix $\tilde{H} \in \mathbb{R}^{X \times Y}$ such that

$$\tilde{H} = \sum_{p=1}^n w_{hc}^p C_t^p \quad (13)$$

Function f (in equation 11) is the implementation of F (in equation 1) for discretized observation maps. As mentioned in section 3, the analytical form of F or f is known to us, but the physical parameters θ are unknown and trainable. Spatial derivatives of observation map U_t are computed as convolution with differential kernels. D_{kl} denotes the differential kernel corresponds to $\frac{\partial^{k+l}}{\partial x^k \partial y^l}$. The size and elements of a differential kernel are determined by the finite difference approximation of corresponding derivative. H_t represents the solution of the system that is governed by a homogenous PDE. In other words, H_t corresponds to the predicted map at timestep t when there is no source term or perturbation.

4.3. Approach to Incorporate Source Dynamics

The basic structure of RNN for homogeneous PDE needs to be modified to incorporate dynamic source term. Figure 2(b) shows the modified structure (PhICNet). An internal state V_t is added in the cell that estimates the perturbation from predicted homogeneous solution from the previous step and the current input. $V_t \in \mathbb{R}^{X \times Y}$ is computed as follows.

$$V_t = U_t - H_{t-1} \quad (14)$$

Finally, the predicted map \hat{U}_{t+1} is computed by the following equation.

$$\hat{U}_{t+1} = H_t + V_t + g(V_t) \quad (15)$$

Function g , the implementation of function G (in equation 2) for discretized source map, captures the source dynamics. We use a residual convolutional network for this purpose such that

$$\hat{V}_{t+1} = V_t + g(V_t) \quad (16)$$

\hat{V}_{t+1} is the predicted source map which is added to the homogeneous solution H_t to get the predicted map \hat{U}_{t+1} (equation 15).

The motivation behind using residual network for modeling the source dynamics is that several studies have established the connection between residual networks and differential equations (Weinan, 2017; Lu et al., 2018; Chang et al., 2018; Chen et al., 2018). We use an architecture similar to residual encoder-decoder network (RED-Net) (Mao et al., 2016). Figure 3 shows the architecture with M convolutional and M transposed convolutional blocks. Each convolutional block consists of two convolutional layers. Similarly, each transposed convolutional block comprises two transposed convolutional layers. Convolutional encoder extracts feature at different scales. These feature maps are used by the transposed convolutional decoder with symmetric skip connections from corresponding convolutional block to capture dynamics at different scales. Skip connection also allows to use deeper network for complex dynamics without encountering the problem of vanishing gradient.

The computation at the m^{th} convolutional block is given by the following equation.

$$\tilde{V}_m = \sigma(W_{m2} * \sigma(W_{m1} * \tilde{V}_{m-1})), \quad m \in \{1, \dots, M\}, \quad \tilde{V}_0 = V_t \quad (17)$$

The computation at the m^{th} transposed convolution block from the end is delineated by the following equation.

$$\tilde{V}'_m = \sigma(W'_{m2} * \sigma(W'_{m1} * \tilde{V}'_{m+1}) + \tilde{V}_{m-1}), \quad m \in \{1, \dots, M\} \quad (18)$$

The predicted source map is given by $\hat{V}_{t+1} = \tilde{V}'_1$. \star denotes the transposed convolution operation and σ is the activation function *relu*.

4.4. Training Loss

For a sequence of observation maps $\{U_0, U_1, \dots, U_T\}$ and n^{th} order (temporal) system, the prediction loss is defined as follows.

$$\mathcal{L}_{pred} = \frac{1}{T-n} \sum_{t=n+1}^T \|U_t - \hat{U}_t\|_2^2 \quad (19)$$

Estimated source map V_t , after observing U_t at timestep t , should match with predicted source map \hat{V}_t from previous

timestep. Accordingly, we add a source prediction loss $\mathcal{L}_{source_pred}$ to the training objective.

$$\mathcal{L}_{source_pred} = \frac{1}{T-n} \sum_{t=n+1}^T \|V_t - \hat{V}_t\|_2^2 \quad (20)$$

Furthermore, source map can be densely distributed or sparse (may contain only a single source). To deal with source map sparsity, we add a $L1$ penalty :

$$\mathcal{L}_{source_sparse} = \frac{1}{T-n} \sum_{t=n+1}^T \|\hat{V}_t\|_1 \quad (21)$$

The overall loss for training is $\mathcal{L} = \mathcal{L}_{pred} + \mathcal{L}_{source_pred} + \lambda \mathcal{L}_{source_sparse}$, where λ is a hyperparameter.

5. Experimental Evaluation

We evaluate our model on two dynamical systems: heat diffusion system and wave propagation system. Heat diffusion system has temporal order of 1, while wave propagation system is a second order system. We compare our model with ConvLSTM (Xingjian et al., 2015), PDE-Net (Long et al., 2018b), a residual encoder-decoder network. As we mentioned before, PDE-Net cannot be used directly for this problem because of the dynamic source term. In original PDE-Net, the authors use polynomial approximation on observed physical quantity to model internal source term. As the source term in our problem is external and dynamic, we perform the polynomial approximation on the difference between two consecutive observation maps and we call this modified model PDE-Net*. In contrast to the residual encoder-decoder used in our model to predict only the source dynamics, the baseline residual encoder-decoder network (RED-Net) models the combined dynamics. Accordingly, the input and output of the baseline residual encoder-decoder network are observation maps (U). We use $M = 3$ for residual encoder-decoder networks. For PDE-Net* and RED-Net baselines, we assume the temporal order of the system is known a priori, i.e. for an n^{th} order system, input to the models is the sequence $\{U_t, U_{t-1}, \dots, U_{t-n}\}$ while predicting \hat{U}_{t+1} . We employ Adam optimizer (with initial learning rate of 0.001) to train the models.

All the models are implemented in PyTorch framework (Paszke et al., 2019). We run all the experiments on a computer equipped with NVIDIA GTX 1080Ti GPU.

5.1. Heat Diffusion System

Heat diffusion at the surface of a material is described by:

$$\frac{\partial u}{\partial t} = \alpha \left(\frac{\partial^2 u}{\partial x^2} + \frac{\partial^2 u}{\partial y^2} \right) + v(x, y, t), \quad (x, y) \in \Omega \subset \mathbb{R}^2, t \in [0, T] \quad (22)$$

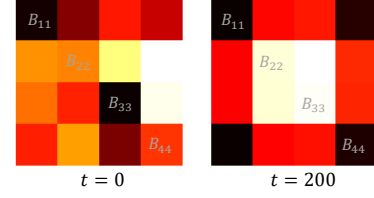


Figure 4. Heat-source maps at the initial and final time step of an example sequence used in our experiment.

where $u(x, y, t)$ is the heat density at location (x, y) at time t and $v(x, y, t)$ is the perturbation due to heat source(s). α is the thermal diffusivity of the material. Equation 22 is one of the fundamental PDEs and is used to describe diffusion of heat, chemicals, brownian motion, diffusion models of population dynamics, and many other phenomena (Strauss, 2007).

The computation space Ω is discretized into 64×64 regular mesh, i.e. $U_t \in \mathbb{R}^{64 \times 64}$. For heat-source, we consider the source map $V_t \in \mathbb{R}^{64 \times 64}$ is divided into 16 equal-sized blocks initialized with random values in $[0, 1]$. All grid points belonging to a block B_{kl} take same value at any time step. The evolution of source map happens in the block level. Each block B_{kl} follows a dynamics given by:

$$\frac{dV_t^{B_{kl}}}{dt} = \sum_{(r,s) \in \mathcal{N}(k,l)} \gamma (V_t^{B_{rs}} - V_t^{B_{kl}}) \quad (23)$$

where $V_t^{B_{kl}}$ denotes the value of block B_{kl} at timestep t , γ is a constant and $\mathcal{N}(k, l)$ represents the 4-connected neighborhood of block B_{kl} . Figure 4 shows an example of source map at the initial and final time step. Training and test dataset are generated using numerical solution method starting from initial condition $U_{t < 0} = 0$ and assuming homogeneous Dirichlet boundary condition. Each sequence is comprises 200 frames and the training set contains 100 such sequences while the test set contains 50.

In this system, the trainable parameters are diffusivity α and the parameters of the residual encoder-decoder network used to model the source dynamics. Since we need second-order spatial derivatives (equation 22), the minimum size of the corresponding differential kernels should be 3×3 . Specifically, following two differential kernels are used to compute H_t in equation 11.

$$D_{20} = \begin{pmatrix} 0 & 0 & 0 \\ 1 & -2 & 1 \\ 0 & 0 & 0 \end{pmatrix}, \quad D_{02} = \begin{pmatrix} 0 & 1 & 0 \\ 0 & -2 & 0 \\ 0 & 1 & 0 \end{pmatrix} \quad (24)$$

We use Signal-to-Noise Ratio (SNR), defined in equation 25, as metric for quantitative comparison among different models and ground truth.

$$SNR(U_t, \hat{U}_t) = 20 \log_{10} \frac{\|U_t\|_2}{\|U_t - \hat{U}_t\|_2} \quad (25)$$

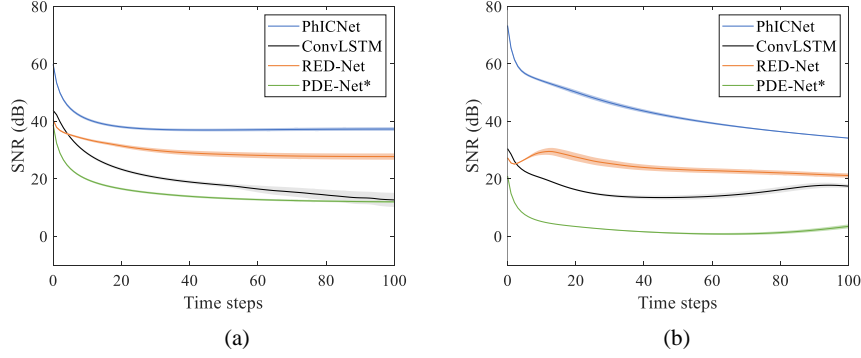


Figure 5. Quantitative (SNR) comparison of forecasting performance of different models for (a) heat diffusion system, (b) wave propagation system. Shaded areas show 95% confidence interval.

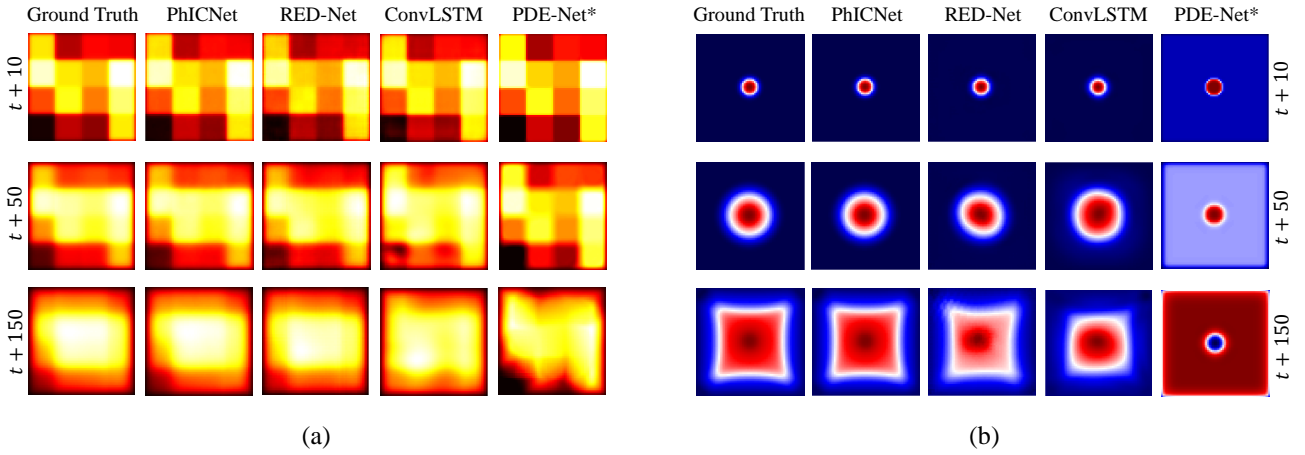


Figure 6. Qualitative comparison of predicted (a) heat maps and (b) wave maps by different models at time steps $t + 10$, $t + 50$ and $t + 150$ when last observation is taken at t .

Figure 5(a) shows the SNR comparison over time steps for the heat diffusion system. Qualitative comparison of predicted heat maps by different models along with ground truth is depicted in Figure 6(a). PhICNet outperforms all the baselines. RED-Net is the best performing baseline. Effective modeling of dynamics by RED-Net is a key factor in the performance of our model as well since we use it for source dynamics modeling. Source maps predicted by our model are compared with ground truth in Figure 7(a).

5.2. Wave Propagation System

Undulation in a stretched elastic membrane due to some perturbation can be described by:

$$\frac{\partial^2 u}{\partial t^2} = c^2 \left(\frac{\partial^2 u}{\partial x^2} + \frac{\partial^2 u}{\partial y^2} \right) + v(x, y, t),$$

$$(x, y) \in \Omega \subset \mathbb{R}^2, t \in [0, T] \quad (26)$$

where $u(x, y, t)$ is the deflection at location (x, y) at time t and $v(x, y, t)$ is the external perturbation. c is the wave propagation speed. We assume a circular perturbation at the center of the membrane which follows a dynamics given by:

$$\frac{dv}{dt} = -\beta v \quad (27)$$

where β is a positive constant.

Similar to heat diffusion system, the computation space Ω is discretized into 64×64 regular mesh, i.e. $U_t \in \mathbb{R}^{64 \times 64}$. Unlike the source map considered for the heat system, the source map $V_t \in \mathbb{R}^{64 \times 64}$ for this wave system is sparse as the perturbation is applied only at a small area at the center. V_0 is initialized with random values in $[1, 2]$. Training and test dataset are generated using numerical solution method starting from initial condition $U_{t < 0} = 0$ and assuming homogeneous Dirichlet boundary condition. Each sequence is comprises 200 frames and the training set contains 100 such sequences while the test set contains 50. Trainable

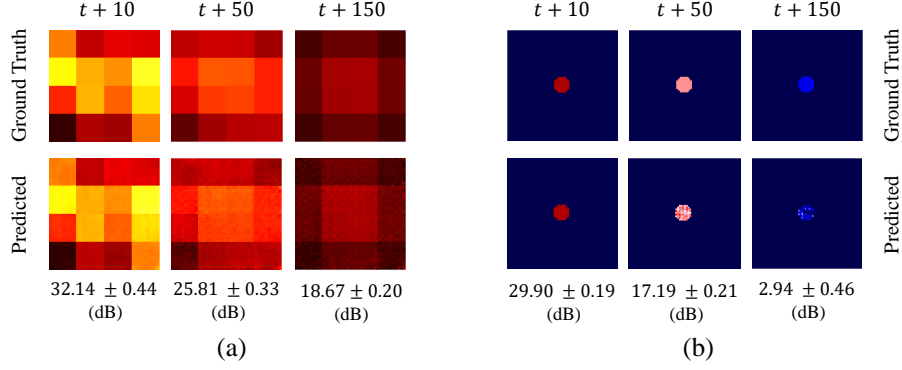


Figure 7. Quantitative and qualitative comparison between true source maps and predicted source maps by PhICNet for (a) heat system and (b) wave system at time steps $t + 10$, $t + 50$ and $t + 150$. SNR values (with 95% confidence interval) are shown at the bottom of predicted source maps.

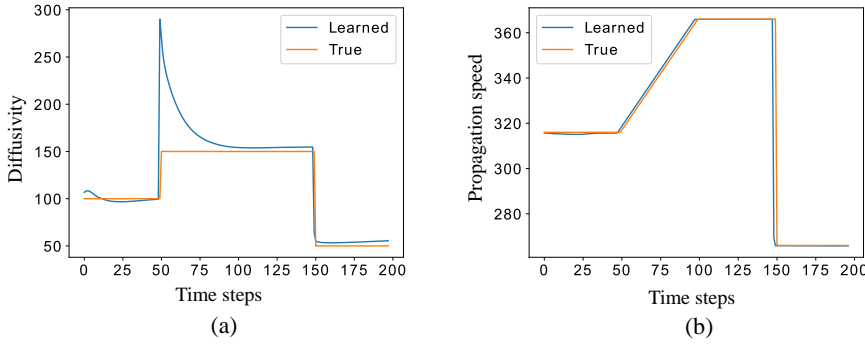


Figure 8. Online learning of time-varying physical parameters: (a) diffusivity of heat diffusion system, (b) propagation speed of wave propagation speed.

parameters for this system include propagation speed c and the parameters of residual encoder-decoder network that is used to model the source dynamics. The differential kernels used for this system are same as equation 24. Quantitative and qualitative performance of different models for wave propagation system are shown in Figure 5(b) and Figure 6(b) respectively. Figure 7(b) compares the source maps predicted by our model with ground truth.

5.3. Online Learning of Time-varying Physical Parameters

In all aforementioned experiments, we have considered unknown but constant physical parameters which are learned in conjunction with unknown source dynamics. However, physical parameters of real-world physical systems are often not fixed and can change over time. In this experiment, we vary the physical parameter of the system over time and investigate if the trained model can adapt with new values of the physical parameter online. At each time step, the current observation is used to re-tune the physical parameters of the

system, while the other parameters are kept frozen. Figure 8 shows that our model can quickly adapt with changes in physical parameters.

6. Conclusion

We developed a physics-incorporated recurrent neural network PhICNet for spatiotemporal forecasting of dynamical systems with time-varying independent source. Besides forecasting the combined dynamics, our model is also capable of predicting the evolution of source dynamics separately. PhICNet is generalized to a class of generic PDEs perturbed with source that follows an independent first-order dynamics. It is possible to incorporate higher order source dynamics by combining estimated source maps from past few time steps for current step prediction of source map. We aim to investigate this as a future work. Furthermore, the assumption on knowledge of analytical form of the underlying PDE can also be relaxed by allowing trainable convolution kernels like PDE-Net.

References

- Chang, B., Meng, L., Haber, E., Ruthotto, L., Begert, D., and Holtham, E. Reversible architectures for arbitrarily deep residual neural networks. In *Thirty-Second AAAI Conference on Artificial Intelligence*, 2018.
- Chen, T. Q., Rubanova, Y., Bettencourt, J., and Duvenaud, D. K. Neural ordinary differential equations. In *Advances in neural information processing systems*, pp. 6571–6583, 2018.
- Chung, J., Gulcehre, C., Cho, K., and Bengio, Y. Empirical evaluation of gated recurrent neural networks on sequence modeling. *arXiv preprint arXiv:1412.3555*, 2014.
- de Bezenac, E., Pajot, A., and Gallinari, P. Deep learning for physical processes: Incorporating prior scientific knowledge. *Journal of Statistical Mechanics: Theory and Experiment*, 2019(12):124009, 2019.
- Finn, C., Goodfellow, I., and Levine, S. Unsupervised learning for physical interaction through video prediction. In *Advances in neural information processing systems*, pp. 64–72, 2016.
- Funahashi, K.-i. and Nakamura, Y. Approximation of dynamical systems by continuous time recurrent neural networks. *Neural networks*, 6(6):801–806, 1993.
- He, K., Zhang, X., Ren, S., and Sun, J. Deep residual learning for image recognition. In *Proceedings of the IEEE conference on computer vision and pattern recognition*, pp. 770–778, 2016.
- Hochreiter, S. and Schmidhuber, J. Long short-term memory. *Neural computation*, 9(8):1735–1780, 1997.
- Kumar, A., Irsoy, O., Ondruska, P., Iyyer, M., Bradbury, J., Gulrajani, I., Zhong, V., Paulus, R., and Socher, R. Ask me anything: Dynamic memory networks for natural language processing. In *International conference on machine learning*, pp. 1378–1387, 2016.
- Lee, N., Choi, W., Vernaza, P., Choy, C. B., Torr, P. H., and Chandraker, M. Desire: Distant future prediction in dynamic scenes with interacting agents. In *Proceedings of the IEEE Conference on Computer Vision and Pattern Recognition*, pp. 336–345, 2017.
- Li, X.-D., Ho, J. K., and Chow, T. W. Approximation of dynamical time-variant systems by continuous-time recurrent neural networks. *IEEE Transactions on Circuits and Systems II: Express Briefs*, 52(10):656–660, 2005.
- Liao, Q. and Poggio, T. Bridging the gaps between residual learning, recurrent neural networks and visual cortex. *arXiv preprint arXiv:1604.03640*, 2016.
- Long, Y., She, X., and Mukhopadhyay, S. Hybridnet: Integrating model-based and data-driven learning to predict evolution of dynamical systems. In *Conference on Robot Learning*, pp. 551–560, 2018a.
- Long, Z., Lu, Y., Ma, X., and Dong, B. Pde-net: Learning pdes from data. In *International Conference on Machine Learning*, pp. 3208–3216, 2018b.
- Long, Z., Lu, Y., and Dong, B. Pde-net 2.0: Learning pdes from data with a numeric-symbolic hybrid deep network. *Journal of Computational Physics*, 399:108925, 2019.
- Lu, Y., Zhong, A., Li, Q., and Dong, B. Beyond finite layer neural networks: Bridging deep architectures and numerical differential equations. In *International Conference on Machine Learning*, pp. 3282–3291, 2018.
- Mao, X., Shen, C., and Yang, Y.-B. Image restoration using very deep convolutional encoder-decoder networks with symmetric skip connections. In *Advances in neural information processing systems*, pp. 2802–2810, 2016.
- Minderer, M., Sun, C., Villegas, R., Cole, F., Murphy, K. P., and Lee, H. Unsupervised learning of object structure and dynamics from videos. In *Advances in Neural Information Processing Systems*, pp. 92–102, 2019.
- Paszke, A., Gross, S., Massa, F., Lerer, A., Bradbury, J., Chanan, G., Killeen, T., Lin, Z., Gimelshein, N., Antiga, L., et al. Pytorch: An imperative style, high-performance deep learning library. In *Advances in Neural Information Processing Systems*, pp. 8024–8035, 2019.
- Pearlmutter, B. A. Learning state space trajectories in recurrent neural networks. *Neural Computation*, 1(2):263–269, 1989.
- Raissi, M. Deep hidden physics models: Deep learning of nonlinear partial differential equations. *The Journal of Machine Learning Research*, 19(1):932–955, 2018.
- Raissi, M. and Karniadakis, G. E. Hidden physics models: Machine learning of nonlinear partial differential equations. *Journal of Computational Physics*, 357:125–141, 2018.
- Raissi, M., Perdikaris, P., and Karniadakis, G. E. Physics informed deep learning (part ii): Data-driven discovery of nonlinear partial differential equations, 2017.
- Robinson, T. An application of recurrent nets to phone probability estimation. *IEEE transactions on Neural Networks*, 5(2), 1994.
- Rudy, S. H., Brunton, S. L., Proctor, J. L., and Kutz, J. N. Data-driven discovery of partial differential equations. *Science Advances*, 3(4):e1602614, 2017.

- Rumelhart, D. E., Hinton, G. E., and Williams, R. J. Learning representations by back-propagating errors. *Nature*, 323(6088):533–536, 1986.
- Schaeffer, H. Learning partial differential equations via data discovery and sparse optimization. *Proceedings of the Royal Society A: Mathematical, Physical and Engineering Sciences*, 473(2197):20160446, 2017.
- Schuster, M. and Paliwal, K. K. Bidirectional recurrent neural networks. *IEEE Transactions on Signal Processing*, 45(11):2673–2681, 1997.
- Strauss, W. A. *Partial differential equations: An introduction*. John Wiley & Sons, 2007.
- Sutskever, I., Vinyals, O., and Le, Q. Sequence to sequence learning with neural networks. *Advances in NIPS*, 2014.
- Trischler, A. P. and DEleuterio, G. M. Synthesis of recurrent neural networks for dynamical system simulation. *Neural Networks*, 80:67–78, 2016.
- Weinan, E. A proposal on machine learning via dynamical systems. *Communications in Mathematics and Statistics*, 5(1):1–11, 2017.
- Werbos, P. J. Backpropagation through time: what it does and how to do it. *Proceedings of the IEEE*, 78(10):1550–1560, 1990.
- Xingjian, S., Chen, Z., Wang, H., Yeung, D.-Y., Wong, W.-K., and Woo, W.-c. Convolutional lstm network: A machine learning approach for precipitation nowcasting. In *Advances in neural information processing systems*, pp. 802–810, 2015.
- Yeo, K. and Melnyk, I. Deep learning algorithm for data-driven simulation of noisy dynamical system. *Journal of Computational Physics*, 376:1212–1231, 2019.
- Yu, R., Zheng, S., Anandkumar, A., and Yue, Y. Long-term forecasting using tensor-train rnns. *arXiv preprint arXiv:1711.00073*, 2017a.
- Yu, R., Zheng, S., and Liu, Y. Learning chaotic dynamics using tensor recurrent neural networks. In *ICML Workshop on Deep Structured Prediction*, volume 17, 2017b.